

Luminescent Dipyrinato Complexes of Trivalent Group 13 Metal Ions

Van S. Thoi, Jay R. Stork, Douglas Magde,* and Seth M. Cohen*

Department of Chemistry and Biochemistry, University of California, San Diego, La Jolla, California 92093-0358

Received August 21, 2006

Although free dipyrins (dipyrromethenes) do not strongly luminesce, certain dipyrinato complexes of BF₂ and zinc(II) are known to be intensely luminescent species. Two new dipyrinato fluorophores, based on complexes with gallium(III) and indium(III), are described. Using a previously described *meso*-mesityl-substituted dipyrin, namely 5-mesityldipyrin (mesdpm), the complexes [Ga(mesdpm)₃] and [In(mesdpm)₃] were prepared and structurally characterized. The complexes display the expected octahedral geometry about the metal ions. In some solvents, such as hexanes, the complexes emit green light upon excitation with UV light at room temperature, with quantum yields of 2.4% ([Ga(mesdpm)₃]) and 7.4% ([In(mesdpm)₃]) and lifetimes in the low nanosecond range. Observations are consistent with assignment to ligand-localized transitions, and this interpretation is further confirmed by density functional calculations described herein. The new complexes are important additions to the widely used family of dipyrin-based fluorescent species and show that dipyrinato complexes containing metals other than BF₂ and zinc(II) may be useful fluorophores.

Introduction

4,4-Difluoro-4-bora-3a,4a-diaza-s-indacene (difluoroborondipyrromethene or BODIPY) dyes represent a group of organic fluorophores widely used in chemical and biochemical investigations (Chart 1).^{1–7} The widespread interest in BODIPY dyes can be attributed to, among other traits, their intense absorption/emission features and photochemical stability. BODIPY dyes were the only fluorescent dipyrin (dipyrromethene) species known for some time until recently, when Lindsey and co-workers showed that a zinc(II) dipyrinato complex, namely [Zn(mesdpm)₂] (mesdpm = 5-mesityldipyrin), was highly emissive ($\Phi_f = 0.36$).⁸ On the basis

of the analysis of several other zinc(II) dipyrinato derivatives, it was determined that restricted rotation of the *meso*-mesityl ring relative to the plane of the dipyrin chromophore was crucial for obtaining good emission from these complexes. This hypothesis was further confirmed in an independent study, where the formation of a rigid, dimeric zinc(II) dipyrinato structure ([Zn₂Cl₂(2-pyrdpm)₂]) also showed enhanced luminescence ($\Phi_f = 0.057$).⁹

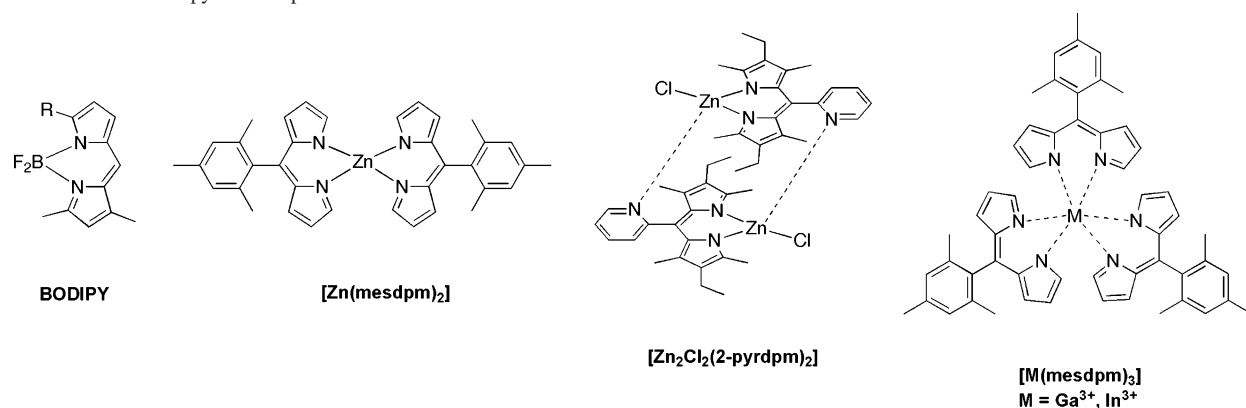
Recently, we have utilized dipyrinato coordination complexes as metalloligands in the preparation of metal-organic frameworks (MOFs).^{10,11} MOFs hold promise as a new family of materials with potential applications in molecular storage, sensors, and catalysis.^{12–14} On the basis of the aforementioned reports, we were intrigued by the possibility of preparing fluorescent MOFs derived from dipyrinato metal complexes; however, the metalloligands utilized in our earlier studies are based on 3-fold symmetric tris(dipyrinato) complexes of iron(III) and cobalt(III), as opposed to the

* To whom correspondence should be addressed. Phone: (858) 822-5596 (S.M.C.). Fax: (858) 822-5598 (S.M.C.). E-mail: scohen@ucsd.edu (S.M.C.).

- (1) Ulrich, G.; Goze, C.; Guardigli, M.; Roda, A.; Ziessel, R. *Angew. Chem., Int. Ed.* **2005**, *44*, 3694–3698.
- (2) Baruah, M.; Qin, W. W.; Basaric, N.; De Borggraeve, W. M.; Boens, N. *J. Org. Chem.* **2005**, *70*, 4152–4157.
- (3) Baruah, M.; Qin, W. W.; Vallee, R. A. L.; Beljonne, D.; Rohand, T.; Dehaen, W.; Boens, N. *Org. Lett.* **2005**, *7*, 4377–4380.
- (4) Basaric, N.; Baruah, M.; Qin, W. W.; Metten, B.; Smet, M.; Dehaen, W.; Boens, N. *Org. Biomol. Chem.* **2005**, *3*, 2755–2761.
- (5) Qin, W. W.; Baruah, M.; Stefan, A.; Van der Ameraer, M.; Boens, N. *ChemPhysChem* **2005**, *6*, 2343–2351.
- (6) Qin, W. W.; Baruah, M.; Van der Auweraer, M.; De Schryver, F. C.; Boens, N. *J. Phys. Chem. A* **2005**, *109*, 7371–7384.
- (7) Zeng, L.; Miller, E. W.; Pralle, A.; Isacoff, E. Y.; Chang, C. J. *J. Am. Chem. Soc.* **2006**, *128*, 10–11.
- (8) Sazanovich, I. V.; Kirmaier, C.; Hindin, E.; Yu, L.; Bocian, D. F.; Lindsey, J. S.; Holtz, D. *J. Am. Chem. Soc.* **2004**, *126*, 2664–2665.

- (9) Sutton, J. M.; Rogerson, E.; Wilson, C. J.; Sparke, A. E.; Archibald, S. J.; Boyle, R. W. *Chem. Commun.* **2004**, 1328–1329.
- (10) Halper, S. R.; Cohen, S. M. *Inorg. Chem.* **2005**, *44*, 486–488.
- (11) Murphy, D. L.; Malachowski, M. R.; Campana, C. F.; Cohen, S. M. *Chem. Commun.* **2005**, 5506–5508.
- (12) Eddaoudi, M.; Moler, D. B.; Li, H.; Chen, B.; Reineke, T. M.; O'Keeffe, M.; Yaghi, O. M. *Acc. Chem. Res.* **2001**, *34*, 319–330.
- (13) Kitagawa, S.; Kitaura, R.; Noro, S. *Angew. Chem., Int. Ed.* **2004**, *43*, 2334–2375.
- (14) Smithenry, D. W.; Suslick, K. S. *J. Porphyrins Phthalocyanines* **2004**, *8*, 182–190.

Chart 1. Fluorescent Dipyrin Compounds.



2-fold symmetric bis(dipyrinato) complexes described with zinc(II). With these ideas in mind, we sought to identify a new class of dipyrin fluorophores based on trivalent cations that would support an octahedral geometry and hence generate a 3-fold symmetric, luminescent metalloligand. We reasoned that the closed-shell d^{10} electron configuration of zinc(II) was likely important to avoid nonradiative deactivation pathways for the dipyrinato excited state. This assumption, combined with the success of the boron-based BODIPY dyes, suggested to us that closed-shell, trivalent Group 13 ions might generate the desired compounds.

The hypothesis that Group 13 cations such as gallium(III) and indium(III) might form emissive tris(dipyrinato) complexes was further supported by literature reports that these ions can generate luminescent porphyrin species. Several studies have reported on the luminescence and photochemistry of porphyrin and phthalocyanine complexes with Group 13 metals.^{15–20} Group 13 tetraphenylporphyrin (TPP) complexes have been reported with quantum yields ranging from 0.0037 to 0.11 in a variety of organic solvents,¹⁵ and phthalocyanine complexes have shown quantum yields up to 0.58.²⁰ Interestingly, in these planar systems, quantum yields follow the trend aluminum(III) > gallium(III) > indium(III). As synthetic progenitors of porphyrins, dipyrinato ligands were anticipated to form Group 13 complexes with interesting photophysical characteristics. Indeed, a prior patent application does make reference to aluminum(III) dipyrinato complexes as fluorophores,²¹ although this document lacks any detailed description of these compounds.

This report discusses the synthesis, structure, and photophysical properties of tris(5-mesityldipyrinato)gallium(III) and tris(5-mesityldipyrinato)indium(III) ($[M(\text{mesdpm})_3]$, $M = \text{Ga}^{3+}, \text{In}^{3+}$). Although not as intense as their boron

difluoride and zinc(II) analogues,⁸ these metal ions do activate the dipyrin fluorophore to produce a visible green emission. These complexes represent the only known dipyrinato fluorophores aside from the boron and zinc(II) adducts. In their present formulation, these metal complexes lack the pendant donor groups to form MOFs, but they demonstrate that such metalloligands can be prepared and appropriately derivatized to obtain a building block with the desired symmetry and fluorescent properties. The complexes described here may find use in self-assembling antenna pigments,^{8,22} light-harvesting complexes,¹ and serve to lay the foundation for the synthesis of luminescent MOFs based on a new family of dipyrinato fluorophores.

Experimental Section

General. Unless otherwise noted, starting materials were obtained from commercial suppliers and used without further purification. 5-Mesityldipyrromethane and 4-cyanophenyldipyrromethane were synthesized according to literature procedures.^{11,23} Mass spectrometry was performed at the University of California, San Diego Mass Spectrometry Facility in the Department of Chemistry and Biochemistry. A ThermoFinnigan LCQ-DECA mass spectrometer was used for ESI or APCI analysis, and the data were analyzed using the Xcalibur software suite. A ThermoFinnigan MAT 900XL mass spectrometer with a fast-atom bombardment (FAB) source was used to acquire the data for the high-resolution mass spectra (HRMS). Infrared spectra were collected on a Mattson Research Series FT-IR instrument (using KBr pellets or NaCl plates, laboratory of Prof. Clifford P. Kubiak) at the Department of Chemistry and Biochemistry, University of California, San Diego. ¹H/¹³C NMR spectra were recorded on Varian FT-NMR spectrometers at the Department of Chemistry and Biochemistry, University of California, San Diego. UV–visible spectra were recorded in hexanes using a Perkin-Elmer Lambda 25 spectrophotometer with the UVWinLab 4.2.0.0230 software package. Absorbance spectra are reported as $\lambda_{\text{max}}/\text{nm}$ ($\epsilon/\text{M}^{-1} \text{cm}^{-1}$).

5-Mesityldipyrin. A solution of 5-mesityldipyrromethane²³ (231 mg, 0.88 mmol) in CH_2Cl_2 (50 mL) was oxidized with 2,3-dicyano-5,6-dichloroparabenzquinone (DDQ, 198 mg, 0.88 mmol) in benzene (25 mL) for 15 min at 0 °C. Once oxidation was complete

- (15) Ohno, O.; Kaizu, Y.; Kobayashi, H. *J. Chem. Phys.* **1985**, *82*, 1779–1787.
 (16) Ebeid, E. M.; Habib, A. M.; Abdel-Kader, M. H.; Yousef, A. B.; Guilard, R. *Spectrosc. Acta* **1988**, *44A*, 127–130.
 (17) Kadish, K. M.; Maiya, G. B.; Xu, Q. *Y. Inorg. Chem.* **1989**, *28*, 2518–2523.
 (18) Ishii, K.; Abiko, S.; Kobayashi, N. *Inorg. Chem.* **2000**, *39*, 468–472.
 (19) Harvey, P. D.; Proulx, N.; Martin, G.; Drouin, M.; Nurco, D. J.; Smith, K. M.; Bolze, F.; Gros, C. P.; Guilard, R. *Inorg. Chem.* **2001**, *40*, 4134–4142.
 (20) Brannon, J. H.; Magde, D. *J. Am. Chem. Soc.* **1980**, *102*, 62–65.
 (21) Toguchi, I.; Ishikawa, H.; Morioka, Y.; Oda, A. *Organic electroluminescent component*; 2000.

- (22) Yu, L. H.; Muthukumar, K.; Sazanovich, I. V.; Kirmaier, C.; Hindin, E.; Diers, J. R.; Boyle, P. D.; Bocian, D. F.; Holten, D.; Lindsey, J. S. *Inorg. Chem.* **2003**, *42*, 6629–6647.
 (23) Laha, J. K.; Dhanalekshmi, S.; Taniguchi, M.; Ambroise, A.; Lindsey, J. S. *Org. Proc. Res. Dev.* **2003**, *7*, 799–812.

(as gauged by TLC), [Cu(acac)₂] (acac = acetylacetonate, 114 mg, 0.44 mmol) was added to the solution and the mixture was stirred for ~4 h at room temperature. The solvent was removed using a rotary evaporator, and the resulting residue was purified by flash column chromatography (SiO₂, CH₂Cl₂) to afford bis(5-mesityldipyrrinato)copper(II) as a red solid after removal of solvent (166 mg, 0.28 mmol). Bis(5-mesityldipyrrinato)copper(II) was dissolved in THF (50 mL) and stirred overnight with KCN (187 mg, 2.8 mmol) in H₂O (20 mL). After the mixture was stirred overnight, the THF was removed using a rotary evaporator, and the free 5-mesityldipyrrin was extracted with 3 × 50 mL CH₂Cl₂ to yield the product as a dark yellow solid (167 mg). Yield: 47% (based on isolated bis(5-mesityldipyrrinato)copper(II)), mp 106–109 °C. ¹H NMR (300 MHz, CDCl₃): δ 7.62 (s, 2H), 6.93 (s, 2H), 6.40 (d, *J* = 4.4 Hz, 2H), 6.33 (d, *J* = 4.4 Hz, 2H), 2.36 (s, 3H), 2.10 (s, 6H). APCI-MS: *m/z* 263.14 [M]⁺, 264.14 [M + H]⁺. HR-EIMS Calcd for C₁₈H₁₈N₂: 262.1465. Found: 262.1464. λ_{abs} (hexanes): 285, 424 nm.

Tris(5-mesityldipyrrinato)gallium(III) ([Ga(mesdpm)₃]). A solution of purified 5-mesityldipyrrin (75 mg, 0.28 mmol) in CH₃CN (5 mL) was stirred with a solution of Ga(NO₃)₃ (23.0 mg, 0.09 mmol) in MeOH (0.5 mL) at room temperature overnight. The mixture was then refrigerated overnight, and an orange precipitate was isolated by vacuum filtration (20 mg). Yield: 26%. mp >260 °C. ¹H NMR (400 MHz, CDCl₃): δ 6.92 (s, 6H), 6.91 (s, 6H), 6.50 (d, *J* = 4.4 Hz, 6H), 6.17 (d, *J* = 3.7 Hz, 6H), 2.36 (s, 9H), 2.08 (s, 18H). FAB-MS: *m/z* 852.1 [M]⁺, 853.1 [M+H]⁺. HR-EIMS Calcd for C₅₄H₅₁N₆Ga: 852.3426. Found: 852.3437. λ_{abs} (hexanes): 448 (87 000), 496 (68 000). λ_{em} (hexanes): 528 nm, Φ_f = 0.024(4).

Tris(5-mesityldipyrrinato)indium(III) ([In(mesdpm)₃]). The same procedure was followed as in the synthesis of tris-(5-mesityldipyrrinato)gallium, utilizing purified 5-mesityldipyrrin (75 mg, 0.28 mmol) and InCl₃ (20 mg, 0.09 mmol), giving the product as a yellow solid (15 mg). Yield: 19%. mp >260 °C. ¹H NMR (400 MHz, CDCl₃): δ 7.15 (s, 6H), 6.90 (s, 6H), 6.53–6.52 (d, *J* = 4.4 Hz, 6H), 6.25–6.24 (d, *J* = 4.4 Hz, 6H), 2.36 (s, 9H), 2.04 (s, 18H). FAB-MS: *m/z* 898.8 [M]⁺. HR-EIMS Calcd for C₅₄H₅₁N₆In: 898.3209. Found: 898.3217. λ_{abs} (hexanes): 444 (117 000), 496 (60 100). λ_{em} (hexanes): 522 nm, Φ_f = 0.074(6).

5-(4'-Cyanophenyl)dipyrrin (4-cydpm). A solution of 5-(4'-cyanophenyl)dipyrrinmethane^{11,23} (254 mg, 1.03 mmol) in CH₂Cl₂ (250 mL) was oxidized with DDQ (234 mg, 1.03 mmol) in benzene (200 mL) for 1.5 h at 0 °C. Once oxidation was complete (as gauged by TLC), the volume was reduced by half on a rotary evaporator, and [Cu(acac)₂] (135 mg, 0.51 mmol) was added to the solution and the mixture was stirred for ~4 h at room temperature. The solvent was removed using a rotary evaporator, and the resulting residue was purified by flash column chromatography (SiO₂, CH₂Cl₂) to afford bis(5-(4'-cyanophenyl)dipyrrinato)copper(II) as a red solid after removal of solvent (229 mg, 0.42 mmol). Bis-(5-(4'-cyanophenyl)dipyrrinato)copper(II) was dissolved in THF (50 mL) and stirred overnight with KCN (375 mg, 5.7 mmol) in H₂O (20 mL). After the mixture was stirred overnight, the THF was removed using a rotary evaporator, and the free 5-(4'-cyanophenyl)dipyrrin was extracted with 3 × 50 mL CH₂Cl₂ to yield a dark brown solid (186 mg). Yield: 73% (based on isolated bis(5-(4'-cyanophenyl)dipyrrinato)copper(II)). ¹H NMR (300 MHz, CDCl₃): δ 7.75 (d, *J* = 7.7 Hz, 2H), 7.67 (s, 2H), 7.61 (d, *J* = 8.2 Hz, 2H), 6.47 (d, *J* = 4.4 Hz, 2H), 6.41 (d, *J* = 4.4 Hz, 6H). APCI-MS: *m/z* 246.2 [M + H]⁺.

Tris(5-(4'-cyanophenyl)dipyrrinato)gallium(III) ([Ga(4-cydpm)₃]). A solution of Ga(NO₃)₃ (66 mg, 0.26 mmol) in MeOH

(30 mL) was added to a solution of 5-(4'-cyanophenyl)dipyrrin (186 mg, 0.75 mmol) in CH₃CN (100 mL), and the solution was heated to reflux overnight. After the removal of the solvent on a rotary evaporator, the remaining solid was triturated with hexanes and an orange precipitate was isolated by vacuum filtration (68 mg). Yield: 33%. ¹H NMR (300 MHz, CDCl₃): δ 7.37 (d, *J* = 8.2 Hz, 6H), 7.55 (d, *J* = 8.2 Hz, 6H), 6.86 (d, *J* = 3.6 Hz, 6H), 6.50 (d, *J* = 4.4 Hz, 6H), 6.29 (d, *J* = 3.9 Hz, 6H). FAB-MS: *m/z* 852.1 [M]⁺, 853.1 [M + H]⁺. λ_{bs}(hexanes): 448, 496 nm.

X-ray Crystallographic Analysis. Single crystals of each compound suitable for X-ray diffraction structural determination were mounted on nylon loops with Paratone oil and were cooled in a nitrogen stream on the diffractometer. Data were collected on either a Bruker AXS or a Bruker P4 diffractometer, each equipped with area detectors. Peak integrations were performed with the Siemens SAINT software package. Absorption corrections were applied using the program SADABS.²⁴ Space group determinations were performed by the program XPREF. The structures were solved and refined with the SHELXTL software package (Sheldrick, G. M. *SHELXTL vers. 5.1 Software Reference Manual*; Bruker AXS: Madison, WI, 1997). [Ga(mesdpm)₃] was solved by direct methods, while [In(mesdpm)₃] and [Ga(4-cydpm)₃] were solved by Patterson methods. All hydrogen atoms were fixed at calculated positions with isotropic thermal parameters, and all non-hydrogen atoms were refined anisotropically unless otherwise noted. X-ray crystallographic data is available from the Cambridge Crystallographic Data Centre (<http://www.ccdc.cam.ac.uk>). Refer to CCDC reference numbers 617591, 617592, and 617593.

Steady-State Fluorescence and Quantum Yield Determinations. Fluorescence spectra were recorded on a Perkin-Elmer LS-55 luminescence spectrometer. Relative fluorescence quantum yields, Φ_f, were determined in hexanes or toluene by the optically dilute method from eq 1,²⁵

$$\Phi_f = \Phi_R \left(\frac{I_R}{I_f} \right) \left(\frac{n_f^2}{n_R^2} \right) \left(\frac{D_f}{D_R} \right) \left(\frac{A_R}{A_f} \right) \quad (1)$$

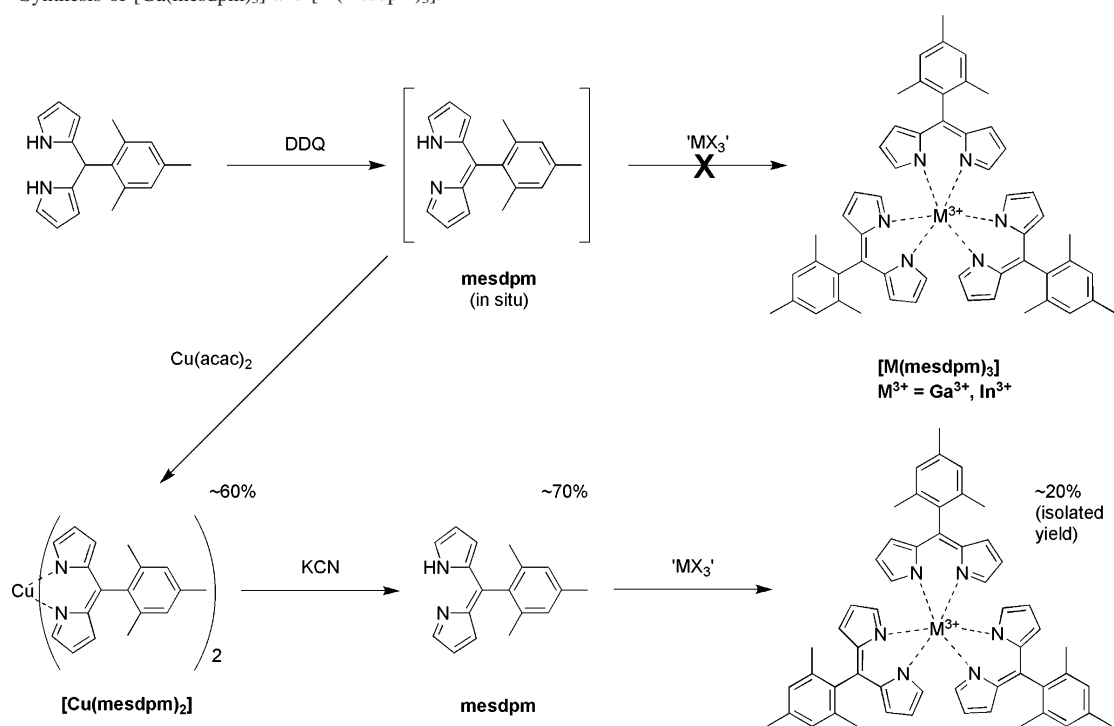
where *I* is excitation intensity, *n* is the refractive index of the solution, *D* is the integrated emission intensity, and *A* is the absorption at the excitation wavelength for the standard reference (R) and sample (f), respectively. Fluorescein in a solution of ethanol and 10⁻⁴ M triethylamine served as the reference (λ_R = 0.91).²⁶ Briefly, for each quantum yield determination, emission spectra of the sample and reference solutions were recorded at the same excitation wavelengths (λ_{ex} = 451 for [Ga(mesdpm)₃]; λ_{ex} = 445 for [In(mesdpm)₃]) using identical instrument configurations to reduce error from instrumental artifacts. Solutions were prepared by adjusting the concentrations of the reference and sample solutions to obtain an absorbance of 0.5 at the desired excitation wavelength. The solutions were then diluted 10-fold to an assumed absorbance of 0.05 before recording emission spectra. At least three independent measurements were made. The emission spectra were integrated with Origin 7.0 software (OriginLab Corporation).²⁷ Excitation spectra were recorded at 530 nm so that there would be additional spectral overlap with the emission spectra. Slits were set at 4.0 (excitation slit) and 4.2 nm (emission slit). The excitation monochromator was scanned from 275 to 520 nm (the sweep width was

(24) Sheldrick, G. M. *Acta Crystallogr., Sect. A* **1995**, *A51*, 33–38.

(25) Demas, J. N.; Crosby, G. A. *J. Phys. Chem.* **1971**, *75*, 991–1024.

(26) Magde, D.; Wong, R.; Seybold, P. G. *Photochem. Photobiol.* **2002**, *75*, 327–334.

(27) *Origin 7.0 SR0*, v7.0220 (B220); OriginLab corporation: Northampton, MA, 1991–2002.

Scheme 1. Synthesis of [Ga(mesdpm)₃] and [In(mesdpm)₃].

truncated to avoid first and second order Rayleigh peaks) with a scan speed of 200 nm/min.

Time-Resolved Measurements. Fluorescence lifetimes were measured by time-correlated photon counting (TCPC). Details of the experimental apparatus and design can be found in the Supporting Information.

Computational Methods. All DFT calculations were performed using the Gaussian 03 package²⁸ on a Linux cluster at the W. M. Keck Laboratory for Integrated Biology II, at the University of California, San Diego. Molecular geometries were optimized in the gas phase with the B3LYP hybrid functional, which incorporates Becke's three-parameter nonlocal exchange potential and the nonlocal correlation functional of Lee, Yang, and Parr.^{29,30} The geometries were initially optimized with the 3-21G* basis set, starting from the crystallographically determined atomic positions for $[\text{Ga}(\text{mesdpm})_3]$, $[\text{In}(\text{mesdpm})_3]$, and bis-(5-phenyldipyrrinato)-zinc(II).²² The *meso*-aryl groups were replaced with hydrogen atoms, thus exchanging the mesdpm ligands with unsubstituted dipyrin (dpm) groups to reduce the computational time. Full optimizations were performed using the 6-31G* basis set for $[\text{Ga}(\text{dpm})_3]$ and $[\text{Zn}(\text{dpm})_2]$ and the LanL2DZ basis set for $[\text{In}(\text{dpm})_3]$, using effective core potentials (ECP) for indium. Molecular structure and orbital drawings were generated with the MOLEKEL program.³¹

Results

Synthesis and Characterization of Dipyrrinato Complexes. Transition metal complexes of α,β -unsubstituted dipyrinato ligands are readily synthesized by complexation

in situ after oxidation of the dipyromethane precursor.^{10,32–35}

The transition metal complexes of these ligands are generally very stable and can be purified by using conventional flash chromatography. Attempts to apply in situ synthetic methods to the Group 13 ions of gallium(III) and indium(III) failed to generate the desired tris(dipyrrinato) complexes (Scheme 1). It became apparent that the gallium(III) and indium(III) complexes, if forming in the oxidation reaction mixture, were not stable to column chromatography. With this obstacle in mind, a new synthetic route to the complexes was required. Because chromatographic purification was not possible, the complexes needed to be prepared from purified dipyrins, so that the complexes could be formed with minimal impurities and isolated by precipitation or crystallization. However, in our experience, free base dipyrins are difficult to isolate in a pure form. A literature report has described isolation of the pure dipyrin by decomposition of the copper(II), zinc(II), and palladium(II) complexes by using 1,4-dithiothreitol (DTT) under neutral conditions.²² Although a versatile procedure, this method proved somewhat cumbersome in our hands and required column chromatography to obtain the desired quantities of purified dipyrin. On the basis of procedures used to remove copper from phenanthroline ligands,^{36,37} a route was devised using KCN to strip copper(II) from the readily purified bis(dipyrrinato)copper(II) complexes. After removal of copper by KCN, the dipyrin

(28) Frisch, M. J.; Trucks, G. W.; Schlegel, H. B.; et al. *Gaussian 03, revision B.04*; Gaussian, Inc.: Wallingford, CT, 2004.

(29) Becke, A. D. *J. Chem. Phys.* **1993**, *98*, 5648–5652.

(30) Lee, C.; Yang, W.; Parr, R. G. *Phys. Rev. B: Condens. Matter Mater. Phys.* **1988**, *37*, 785–789.

(31) Flukiger, P.; Luthi, H. P.; Portmann, S.; Weber, J. *Molekul 4.3*; Swiss Center for Scientific Computing: Manno, Switzerland, 2000–2002.

(32) Brückner, C.; Karunaratne, V.; Rettig, S. J.; Dolphin, D. *Can. J. Chem.* **1996**, *74*, 2182–2193.

(33) Brückner, C.; Zhang, Y.; Rettig, S. J.; Dolphin, D. *Inorg. Chim. Acta* **1997**, *263*, 279–286.

(34) Cohen, S. M.; Halper, S. R. *Inorg. Chim. Acta* **2002**, *341*, 12–16.

(35) Halper, S. R.; Cohen, S. M. *Chem.—Eur. J.* **2003**, *9*, 4661–4669.

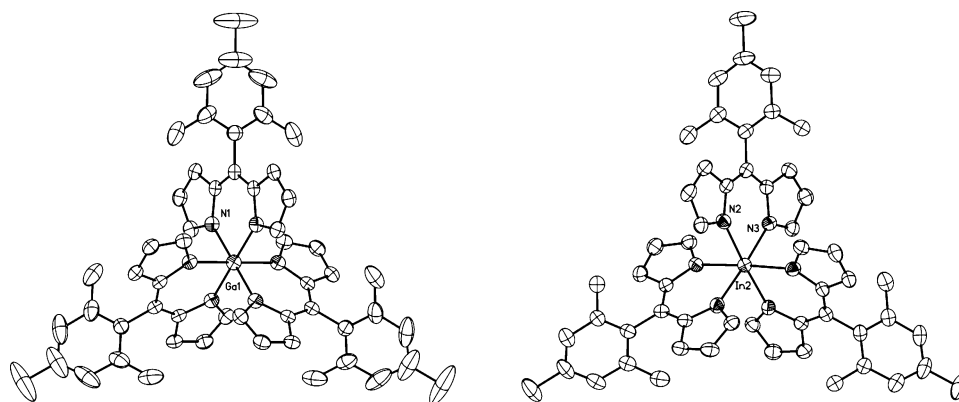
(36) Chambron, J.-C.; Sauvage, J.-P. *J. Am. Chem. Soc.* **1997**, *119*, 9558–9559.

(37) Sauvage, J.-P. *Acc. Chem. Res.* **1990**, *23*, 319–327.

Table 1. X-ray Crystallographic Data for [Ga(4-cydpdm)₃], [Ga(mesdpm)₃], and [In(mesdpm)₃]

	[Ga(4-cydpdm) ₃]	[Ga(mesdpm) ₃]	[In(mesdpm) ₃]
empirical formula	C _{48.83} H _{30.83} Cl _{2.49} GaN ₉ O _{0.25}	C ₅₅ H ₅₂ Cl ₃ GaN ₆	C ₅₅ H _{52.50} InN _{6.50}
cryst syst	triclinic	trigonal	trigonal
space group	<i>P</i> $\bar{1}$	<i>P</i> 3 <i>c</i> 1	<i>P</i> 3 <i>c</i> 1
	unit cell dimensions		
<i>a</i>	14.696(4) Å	23.338(3) Å	23.7036(12) Å
<i>b</i>	16.567(4) Å	23.338(3) Å	23.7036(12) Å
<i>c</i>	20.069(5) Å	15.406(4) Å	14.7117(15) Å
α	95.906(4)°	90°	90°
β	110.802(4)°	90°	90°
γ	106.542(4)°	120°	120°
<i>V</i> , <i>Z</i>	4264(2) Å ³ , 4	7267(2) Å ³ , 6	7158.5(9) Å ³ , 6
cryst size	0.41 × 0.13 × 0.09 mm ³	0.42 × 0.15 × 0.10 mm ³	0.28 × 0.07 × 0.07 mm ³
color and habit	orange needle	orange needle	orange needle
<i>T</i> (K)	100(2)	100(2)	100(2)
reflns collected	36 836	59 678	61 573
independent reflns	17 265 [<i>R</i> (int) = 0.0352]	4948 [<i>R</i> (int) = 0.0344]	4891 [<i>R</i> (int) = 0.0681]
data/restraint/params	17 265/0/1129	4948/6/316	4891/21/317
GOF on <i>F</i> ²	1.022	1.046	1.033
final <i>R</i> indices <i>I</i> > 2σ(<i>I</i>) ^a	<i>R</i> 1 = 0.0462 <i>wR</i> 2 = 0.1093	<i>R</i> 1 = 0.0448 <i>wR</i> 2 = 0.1089	<i>R</i> 1 = 0.0411 <i>wR</i> 2 = 0.0933
<i>R</i> indices (all data) ^a	<i>R</i> 1 = 0.0622 <i>wR</i> 2 = 0.1188	<i>R</i> 1 = 0.0532 <i>wR</i> 2 = 0.1152	<i>R</i> 1 = 0.0798 <i>wR</i> 2 = 0.1099

$$^a R1 = \sum ||F_o| - |F_c|| / \sum |F_o|, wR2 = \{ \sum [w(F_o^2 - F_c^2)^2] / \sum [wF_o^4] \}^{1/2} Z.$$

**Figure 1.** X-ray structures (50% probability ellipsoids) of [Ga(mesdpm)₃] (left) and [In(mesdpm)₃] (right). Hydrogen atoms and solvent molecules have been omitted for clarity.

can be separated and isolated in high yield using a simple extraction. As outlined in Scheme 1, this method is straightforward, and we believe will be applicable to a variety of dipyrrens, providing the purified dipyrren ligands without requiring any additional chromatography.

Using the purified 5-mesityldipyrren, the gallium(III) and indium(III) complexes were prepared by mixing 3 equiv of the ligand with 1 equiv of the appropriate metal salt in a MeOH/CH₃CN solvent mixture. UV–visible spectroscopy shows the reaction to be essentially quantitative; however, isolation/recrystallization of the product proved to be challenging. The MeOH/CH₃CN solvent mixture was selected to maximize precipitation of the product from the reaction mixture, which was vacuum filtered to obtain the pure complexes in relatively low isolated yields (~20–25%). The solubility of the complexes depends on the meso substituent on the dipyrren ligand. Therefore, different precipitation/isolation procedures will likely be required for other tris(dipyrrenato) complexes of this type (e.g., see synthesis of [Ga(4-cydpdm)₃]). Optimization of these isolation procedures

is ongoing. Nevertheless, sufficient quantities of the complexes could be isolated for further characterization and study.

Structures of Complexes. The compounds [Ga(mesdpm)₃], [In(mesdpm)₃], and [Ga(4-cydpdm)₃] were crystallized and examined by single-crystal X-ray crystallography. Crystal data are given in Table 1. In all cases, the dipyrren ligand was similar to those in other dipyrrenato metal complexes that lack pyrrole substituents.^{22,32–35,38–40} [Ga(mesdpm)₃] crystallized as orange needles by slow evaporation from a solution of the complex in deuterated chloroform (Figure 1). The selected crystal was twinned by a 180° rotation about the [2 1 0] reciprocal axis. The asymmetric unit consists of two independent, partial complexes each residing on a special position. One of the two partial complexes includes a gallium atom and a single mesdpm

- (38) Halper, S. R.; Cohen, S. M. *Angew. Chem., Int. Ed.* **2004**, *43*, 2385–2388.
 (39) Gill, H. S.; Finger, I.; Bozidarevic, I.; Szydlo, F.; Scott, M. J. *New J. Chem.* **2005**, *29*, 68–71.
 (40) Do, L.; Halper, S. R.; Cohen, S. M. *Chem. Commun.* **2004**, 2662–2663.

ligand, while the other partial complex presents a gallium(III) ion and one-half of a mesdpm ligand. The full complexes are generated by crystallographically imposed symmetry. A half-occupied, deuterated chloroform solvent molecule is also present and disordered over a special position. Selected bond distances and angles are provided in Figure S1.

The gallium(III) ion in $[\text{Ga}(\text{mesdpm})_3]$ is octahedrally coordinated to the pyrrole nitrogen atoms of three chelating mesdpm ligands. The Ga–N distances of 2.054(2) and 2.055(2) Å are quite similar to the Ga–N distances of 2.054, 2.056, and 2.068 Å found in tris(2,2'-bipyridine)gallium(III) triiodide⁴¹ and are comparable to those of other six-membered gallium(III) metallocycles (Ga–N distance of 2.02(7) Å) identified by a search in the Cambridge Structural Database (CSD).⁴² A separate CSD search for gallium(III) porphyrin compounds uncovered a mean Ga–N distance of 2.04(2) Å. The N–Ga–N angles within the Ga(mesdpm) metallocycles are 89.04(12)° and 89.07(8)°. These angles are slightly less acute than the 87.37° mean N–Ga–N angles of gallium(III) porphyrins. However, it should be noted that the metal is displaced from the mean porphyrin plane in most gallium(III) porphyrin compounds, thus reducing the bite angle.^{17,19,43–50} The dipyrin moieties are essentially planar, with the largest deviation having an angle of 3.4(2)° between the least squares planes of the pyrroles. As would be expected, the mesityl groups are approximately orthogonal to the planar dipyrin moieties. The dihedral angles between the mesityl groups and the metallocycles are 79.90(9)° and 86.02(8)°, respectively. The closest non-hydrogen distance between ligands of a single complex is 3.040 Å between an α -carbon atom of one dipyrin ligand and a nitrogen atom of a neighboring ligand.

Slow diffusion of hexanes into an acetonitrile solution of $[\text{In}(\text{mesdpm})_3]$ produced orange needles of the complex as the acetonitrile solvate (Figure 1). The asymmetric unit is nearly identical to that of $[\text{Ga}(\text{mesdpm})_3]$ and is comprised of 1/3 of one $[\text{In}(\text{mesdpm})_3]$ complex and 1/6 of another. The structure also includes a partially occupied acetonitrile molecule, which is disordered over a glide plane. Selected bond distances and angles are provided in Figure S2. As in $[\text{Ga}(\text{mesdpm})_3]$, the central indium(III) ion of $[\text{In}(\text{mesdpm})_3]$

is octahedrally coordinated to the pyrrolic nitrogen atoms of three chelating mesdpm ligands. The In–N distances are 2.212(3) Å for one complex and 2.215(3) and 2.219(3) Å for the other. These distances are generally intermediate between the In–N distances found in indium porphyrin complexes and complexes of indium with 2,2'-bipyridine. In the former, In–N distances range from 2.125 to 2.212 Å, while in the latter case, the In–N distances range from 2.233 to 2.385 Å.⁴² The N–In–N angles within the metallocycles of $[\text{In}(\text{mesdpm})_3]$ are 84.54(15)° and 84.08(10)°, slightly more acute than the similar angles seen in $[\text{Ga}(\text{mesdpm})_3]$, but in keeping with the larger covalent radius of indium(III). The dipyrin moieties are nearly planar with angles between the least squares planes of the pyrroles of 2.8(3)° and 4.0(3)°. As in $[\text{Ga}(\text{mesdpm})_3]$, the mesityl groups are nearly orthogonal to the dipyrin moieties, with dihedral angles of 79.9(3)° and 84.79(10)°. The closest non-hydrogen distance between ligands of a single complex is 3.295 Å.

Diffraction-quality, orange needles of $[\text{Ga}(4\text{-cydpm})_3]$ were prepared by vapor diffusion of pentane into a chloroform solution of the compound. Two independent, full complexes make up the asymmetric unit. The compound crystallized with two partially occupied chloroform solvent molecules and several partially occupied water molecules. The $[\text{Ga}(4\text{-cydpm})_3]$ complexes are structurally quite similar to $[\text{Ga}(\text{mesdpm})_3]$. Selected bond distances and angles are provided in the Supporting Information (Figure S3). The average Ga–N distance in $[\text{Ga}(4\text{-cydpm})_3]$ is 2.053 Å. The dihedral angles between the phenyl rings and the metallocycles average 69.5° and range from 60.3° to 86.3°, reflecting the loss of steric crowding that results from replacing the mesityl groups with 4-cyanophenyl substituents.

Electronic Spectroscopy. The solution absorption spectra of $[\text{Ga}(\text{mesdpm})_3]$, $[\text{In}(\text{mesdpm})_3]$, and $[\text{Ga}(\text{cydpm})_3]$ are very similar to each other. In addition to several complex, weak, high-energy transitions, the primary spectral feature in all three is an intense ($\epsilon \approx 70\,000\text{--}120\,000\text{ M}^{-1}\text{ cm}^{-1}$), split peak with maxima at about 450 and 500 nm (Figure 2). The apparently vibronic structure ($\epsilon \approx 2300\text{ cm}^{-1}$) in this low-energy feature of all three spectra is considerably more pronounced than that found in $[\text{Zn}(\text{mesdpm})_2]$,⁸ the absorption spectrum of which features a relatively weak, high-energy shoulder ($\epsilon \approx 900\text{ cm}^{-1}$).

Solutions of $[\text{Ga}(\text{cydpm})_3]$ were not noticeably luminescent when irradiated with a hand-held UV lamp ($\lambda_{\text{ex}} = 365\text{ nm}$) or when examined using a spectrofluorimeter ($\lambda_{\text{ex}} = 465\text{ nm}$) and were omitted from further luminescence studies. The uncorrected, steady-state emission spectra of $[\text{Ga}(\text{mesdpm})_3]$ and $[\text{In}(\text{mesdpm})_3]$ in hexanes or dichloromethane solutions, presented in Figure 3, feature a single band that closely mirrors the lower-energy feature of the absorption spectra. The weak vibronic structure noted in the emission spectrum of $[\text{Zn}(\text{mesdpm})_2]$ ⁸ is not apparent in the emission spectra of $[\text{Ga}(\text{mesdpm})_3]$ and $[\text{In}(\text{mesdpm})_3]$. However, the excitation spectra when monitoring the emission at $\lambda_{\text{em}} = 451\text{ nm}$ for $[\text{Ga}(\text{mesdpm})_3]$ and 448 nm for $[\text{In}(\text{mesdpm})_3]$ are virtually identical to the absorption spectra; the emission

(41) Baker, R. J.; Jones, C.; Kloth, M.; Mills, D. P. *New J. Chem.* **2004**, 28, 207–213.

(42) Allen, F. H. *Acta Crystallogr., Sect. B: Struct. Sci.* **2002**, B58, 380–388.

(43) Brancato-Buentello, K. E.; Coutsolelos, A. G.; Scheidt, W. R. *Acta Crystallogr., Sect. C: Cryst. Struct. Commun.* **1996**, 52, 2707–2710.

(44) Okamura, T.; Nishikawa, N.; Ueyama, N.; Nakamura, A. *Chem. Lett.* **1998**, 199–200.

(45) Balch, A. L.; Hart, R. L.; Parkin, S. *Inorg. Chim. Acta* **1993**, 205, 137–143.

(46) Parzuchowski, P. G.; Kampf, J. W.; Rozniecka, E.; Kondratenko, Y.; Malinowska, E.; Meyerhoff, M. E. *Inorg. Chim. Acta* **2003**, 355, 302–313.

(47) Hsieh, Y.-Y.; Sheu, Y.-H.; Liu, I.-C.; Lin, C.-C.; Chen, J.-H.; Wang, S.-S.; Lin, H.-J. *J. Chem. Cryst.* **1996**, 26, 203–207.

(48) Coutsolelos, A. G.; Guillard, R.; Boukhris, A.; Lecomte, C. *J. Chem. Soc., Dalton Trans.* **1986**, 1779–1783.

(49) Boukhris, A.; Lecomte, C.; Coutsolelos, A. G.; Guillard, R. *J. Organomet. Chem.* **1986**, 303, 151–165.

(50) Kadish, K. M.; Cornillon, J.-L.; Korp, J. D.; Guillard, R. *J. Heterocycl. Chem.* **1989**, 26, 1101–1104.

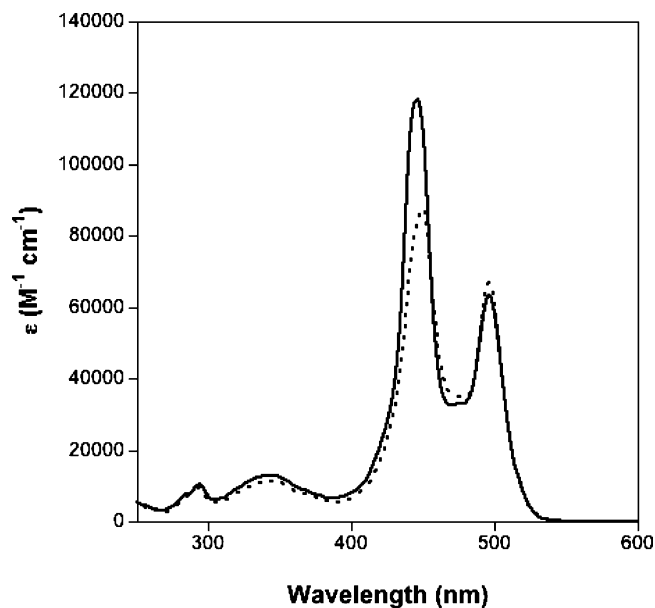


Figure 2. UV–visible spectra of [Ga(mesdpm)₃] (dotted line) and [In(mesdpm)₃] (solid line) in hexanes.

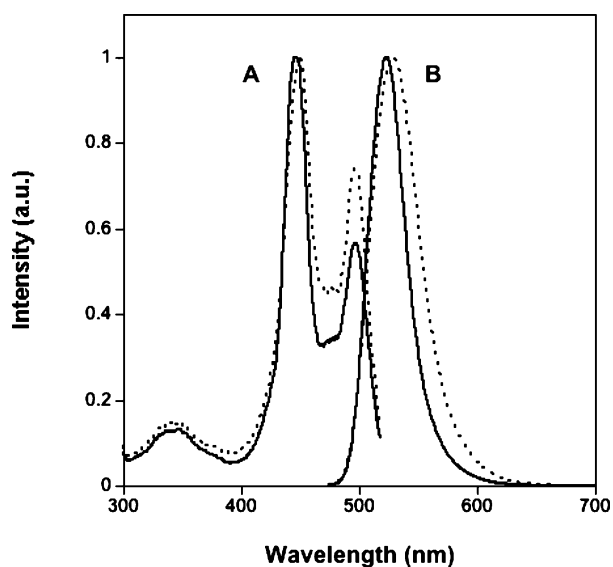


Figure 3. Normalized excitation (A) and emission (B) spectra of $\sim 1 \mu\text{M}$ [Ga(mesdpm)₃] (dotted line) and [In(mesdpm)₃] (solid line) in hexanes. The samples were excited at 451 nm for [Ga(mesdpm)₃] and 448 nm for [In(mesdpm)₃]. Excitation spectra were monitored at 530 nm.

spectrum of [In(mesdpm)₃] is essentially unchanged whether the compound is excited at 365, 448, or 496 nm (Figure S4).

With a fluorescence quantum yield (Φ_f) of 0.074, the emission of [In(mesdpm)₃] in hexanes is more intense than that of [Ga(mesdpm)₃] in the same solvent ($\Phi_f = 0.024$). By comparison, both Group 13 complexes are markedly less luminescent than [Zn(mesdpm)₂] ($\Phi_f = 0.36$ in toluene).⁸ The considerable Stokes shifts (1220 and 1113 cm^{-1} for [Ga(mesdpm)₃] and [In(mesdpm)₃], respectively) and high molar absorptivity, as well as the closed-shell electronic configurations of the central metal atoms, suggest that the most prominent electronic transitions are ligand-centered.

Time-Resolved Fluorescence. Fluorescence decay measurements by TCPC were employed to characterize two completely independent preparations of [Ga(mesdpm)₃] along

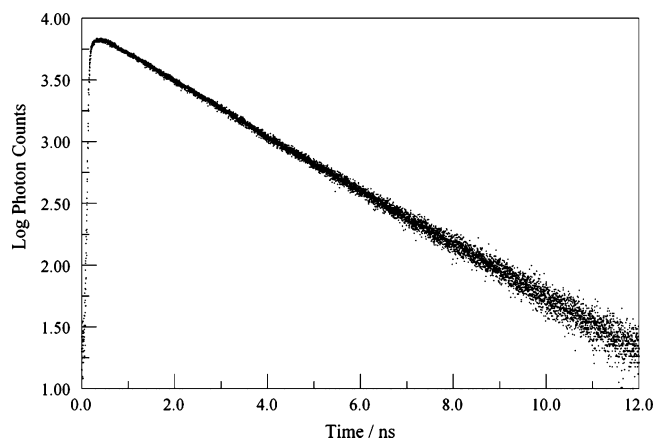


Figure 4. Semilog plot of luminescence decays for [In(mesdpm)₃] in mixed hexanes, showing an overlay of normalized decay curves collected at 500, 530, 560, and 590 nm. All are identical and all are clean, single exponential decays.

with [In(mesdpm)₃], [Zn(mesdpm)₂], and the free ligand (mesdpm). Solvents explored included dichloro-, trichloro-, tribromo-, and tetrachloromethane, acetonitrile, tetrahydrofuran, toluene, methylcyclohexane, and mixed hexanes. Fluorescence decays proved to be highly diagnostic for two reasons. First, TCPC is immune to drift in most experimental parameters and highly linear over many half-lives and thus able to distinguish multiple decays. Second, we were using an excitation wavelength near 400 nm, which is a minimum in the excitation spectra of the complexes (Figure 4). Normally, one might prefer to excite at an absorption maximum to avoid complications by impurities or degradation products. However, excitation at an absorption minimum is more useful for detecting impurities or degradation products.

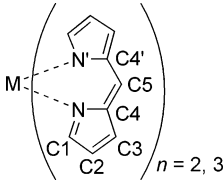
Solutions of the free ligand displayed a short lifetime (about 16 ps) in all solvents, along with less than 1% of a long-lived (3–3.5 ns) component that was not investigated further. In all solvents investigated, except methylcyclohexane and mixed hexanes, all the metal complexes likewise showed a very similar, fast decay, varying in amplitude (10–80%), along with two or more additional decay components in the nanosecond range. This may be due to rapid solvolysis that generates a mixture of metal species, together with the free ligand. Among the solvents for which additional decay components were observed, this behavior was least prominent in toluene but was still quite evident from the data. In addition to immediate solvolysis, there were further degradation processes that could be observed when the liquid solutions were left in the dark for a week or more and re-examined. These further changes resulted in more of the very fast component, and some evolution of the slower decays with no obvious pattern. As to variations of possible solvolysis reactions for different metals, only in the case of toluene was the reaction small enough to permit any conclusion to be drawn. For toluene, [Zn(mesdpm)₂] showed more degradation than did the [Ga(mesdpm)₃] or [In(mesdpm)₃]. In fact, the [Zn(mesdpm)₂] sample showed degradation after one week even in hexanes and methylcyclohexane. By this measure, [Ga(mesdpm)₃] and [In(mesdpm)₃] are even more stable in noncoordinating solvents than

Table 2. Optical Properties of the Lowest Excited Electronic State of Dipyrrinato Metal Complexes in Mixed Hexanes Solvent

metal	$\lambda_{a,max}$ nm	ϵ_{max}^b M ⁻¹ cm ⁻¹	τ_{rad} (predicted) ns	$\lambda_{f,max}$ nm	ϕ	τ_f ns	τ_{rad} ns
Ga	496	68 000	12	528	0.024 ± 0.004	3.75 ± 0.02	156
In	496	60 100	14	522	0.074 ± 0.006	1.93 ± 0.02	26
Zn	487 ^a	115 000 ^a	~6	501	0.36 ^a	3.51 ± 0.04	~10

^a From ref 8. ^b For the lowest-energy peak.

Table 3. Average Structural Parameters (in Å and Degrees) for the Experimental and Calculated Structures

	[Ga(dpm) ₃]		[In(dpm) ₃]		[Zn(dpm) ₂]	
	exptl ^a	B3LYP/ 6-31G*	exptl ^a	B3LYP/ LanL2DZ	exptl ^b	B3LYP/ 6-31G*
M–N	2.054	2.059	2.215	2.208	1.979	1.995
N–C1	1.340	1.338	1.337	1.360	1.338	1.339
C1–C2	1.407	1.417	1.402	1.430	1.408	1.417
C2–C3	1.370	1.383	1.375	1.398	1.369	1.384
C3–C4	1.429	1.425	1.431	1.439	1.419	1.426
C4–N	1.395	1.395	1.392	1.415	1.399	1.397
C4–C5	1.400	1.392	1.403	1.402	1.399	1.396
N–M–N	89.06	90.13	84.31	86.46	94.45	96.37
N–C1–C2	111.6	111.7	111.8	111.4	111.5	111.7
C1–C2–C3	106.5	106.1	106.3	106.3	106.1	106.0
C2–C3–C4	107.1	106.8	107.1	107.1	107.8	107.0
C3–C4–N	108.4	109.0	108.2	108.7	108.0	108.8
C4–N–C1	106.3	106.4	106.6	106.5	106.6	106.5
N–C4–C5	124.8	124.6	125.4	125.3	124.6	124.6
C4–C5–C4'	126.4	127.9	128.0	129.3	127.2	129.4

^a Experimental values are derived from the crystal structures of [Ga(mesdpm)₃] and [In(mesdpm)₃] (this work). ^b Experimental values for [Zn(dpm)₂] are from the crystal structure of bis-(5-phenyldipyrrinato)-zinc(II).²²

the previously reported [Zn(mesdpm)₂]. The gallium(III) and indium(III) complexes are quite stable in hexanes and methylcyclohexane; for these complexes, only single exponential decays (Figure 4) were observed even after solutions were kept at ambient conditions, in low light, for several weeks.

All the measurements that yielded single-exponential fits are reported in the Supporting Information (Table S1). These include the solutions described above at four different wavelengths each. For most samples, the liquid solutions were kept for several weeks in the dark and re-evaluated weekly; the results are listed in chronological order to convey reproducibility. The lifetimes in hexanes may be compared with lifetimes in methylcyclohexane. For [Ga(mesdpm)₃], the fluorescent lifetimes are $\tau_f = 3.747 \pm 0.009$ ns in hexanes and 3.758 ± 0.008 ns in methylcyclohexane. For [In(mesdpm)₃], $\tau_f = 1.929 \pm 0.012$ ns in hexanes and 1.815 ± 0.019 ns in methylcyclohexane. In these four cases, the uncertainties quoted represent 99% confidence intervals calculated using Student's *t*-factors from the data listed. It appears likely that there is a small, but real, difference between solvents. The lifetimes reported in Table 2 are also means of the pertinent data in Table S1, although the uncertainties in Table 2 are increased arbitrarily by a small amount to be even more conservative.

Flash Photolysis. Flash photolysis measurements were carried out for the free ligand, [Ga(mesdpm)₃], [In(mesdpm)₃], and [Zn(mesdpm)₂] for samples prepared in an ambient atmosphere, purged with argon for 30 min, or

oxygenated at 1 atm dioxygen for 30 min. Both ground-state bleaching and excited-state transient absorption could be detected in all cases. The free ligand showed a long-lived transient with lifetime in the range 6–10 ms, with little or no dioxygen dependence. Small features decaying more rapidly could be detected in the air and dioxygen samples, but no such decays could be detected in the argon-purged case. The metal complexes showed transients with lifetimes of 300–320 ns in air, 56–62 ns in 1 atm dioxygen, and 45–80 μ s in the argon-purged case, along with small amounts of a much longer-lived component. The behavior of [Zn(mesdpm)₂] appeared similar to [Ga(mesdpm)₃] and [In(mesdpm)₃].

DFT Calculations. The optimized geometries of [Ga(dpm)₃], [In(dpm)₃], and [Zn(dpm)₃] (dpm = dipyrromethene) were in reasonably good agreement with the structures of the parent compounds [Ga(mesdpm)₃], [In(mesdpm)₃], and bis-(5-phenyldipyrrinato)zinc(II).²² A comparison of structural parameters is provided in Table 3. Most calculated bond distances were within 0.01 Å of the corresponding distances from the X-ray structures. Discrepancies in the C2–C3 distances may have resulted from the replacement of the mesityl groups by hydrogen atoms in the computational studies. The [Zn(dpm)₂] complex was also optimized with the LanL2DZ basis set; however, the bond distances so obtained were consistently longer than the crystallographically determined distances by about 0.05 Å. It is probable that a further geometry optimization of the [In(dpm)₃] complex by applying larger basis sets would improve the

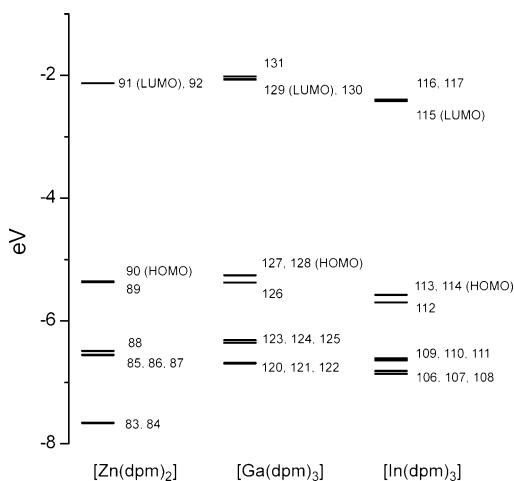


Figure 5. Partial calculated energy level diagrams for [Zn(dpm)₂], [Ga(dpm)₃], and [In(dpm)₃] (dpm = dipyrin).

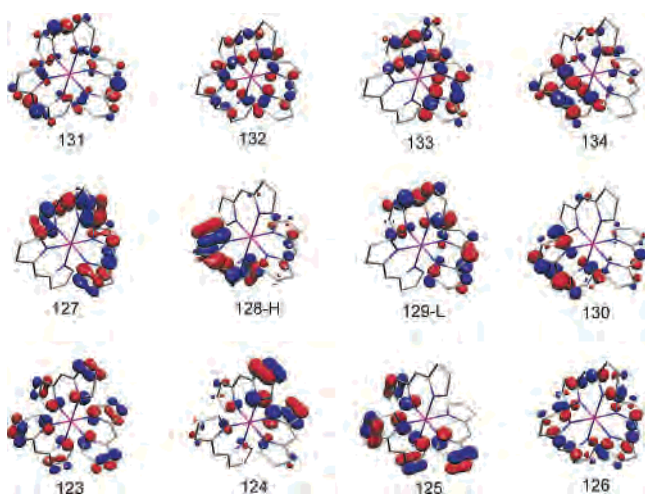


Figure 6. Drawings of the frontier orbitals calculated for [Ga(dpm)₃].

agreement between the computed and experimental bond parameters. A partial energy level diagram is presented in Figure 5. The most likely low-energy electronic transitions are ligand-centered, $\pi \rightarrow \pi^*$ excitations, as can be seen from the frontier molecular orbitals calculated for [Ga(dpm)₃] shown in Figure 6. Frontier molecular orbitals calculated for [In(dpm)₃] and [Zn(dpm)₂] are provided in the Supporting Information (Figures S5 and S6).

Discussion

The three new complexes presented here are the first well-characterized gallium(III) and indium(III) complexes of α,β -unsubstituted dipyrinato ligands. Notably, [Ga(mesdpm)₃] and [In(mesdpm)₃] exhibit luminescence in the visible region when excited by UV light. The optical properties of the lowest excited electronic state in these complexes appear very much as was expected for a ligand-localized transition in a metal complex. The molar absorptivity values are too large to be anything else, and this assertion is also supported by DFT calculations, which indicate that the frontier orbitals are exclusively ligand-centered. For [Ga(mesdpm)₃] or [In(mesdpm)₃], coordination to the metal results in an intensified, red-shifted, split feature compared to the lowest

absorption of the free ligand. This may involve excitonic splitting of the lowest energy transition of the free ligand. For [Zn(mesdpm)₂], the spectrum is rather different and has been considered a single state with a vibrational feature on the blue end of the spectrum.²² The emission from [Ga(mesdpm)₃] or [In(mesdpm)₃] is a mirror image of the lower of the two prominent absorption bands. The fluorescent state has a lifetime of a few nanoseconds and a quantum yield of several percent. All of this proves that the emission is spin-allowed fluorescence from a state that behaves like an organic moiety. A Strickler–Berg analysis^{51,52} including only the lower absorption feature predicts radiative lifetimes as given in Table 2. Nonradiative decay pathways reduce the state lifetime below this value. The actual state lifetime divided by the quantum yield gives a measured radiative lifetime, also displayed in Table 2. Best agreement between prediction and measurement is expected when the absorption is very strong and the molecule is very rigid and undergoes no change in geometry in the excited state. Although large geometry changes were not expected in these molecules, if the interpretation of excitonic coupling (between two or more of the ligands bound to the metal center) is valid, then that coupling is likely to be extremely sensitive to even small changes. For reasons not yet clear, there is a large discrepancy in the predicted and measured lifetimes for [Ga(mesdpm)₃].

The moderately low quantum yields for emission prove that the dominant decay pathways are nonradiative. The flash photolysis results reported above provide convincing evidence that at least a portion of the decay is to a triplet, for we measured transient features with appropriate lifetimes that were strongly dependent on dioxygen concentration. The transient features for [In(mesdpm)₃] appeared slightly more intense, consistent with a normal heavy-atom effect on intersystem crossing to the triplet state. We have no measurement of ground-state repopulation on the time scale of emission, but it is likely that there is also internal conversion to the ground state, as Lindsey and Holten and their collaborators reported.²² This internal conversion may be as much as 70% for the [Zn(mesdpm)₂] complex. Lindsey et al. further reported that, in a different, shorter-lived, weakly fluorescent complex, internal conversion was substantially higher.⁸ This is plausible, as the intersystem crossing rate may well be more or less constant, while internal conversion is the process that produces very short lifetimes. This is consistent with our observation of very weak triplet features in the free ligand. There is also a photochemical process that produces a longer-lived product (several milliseconds), but we do not conjecture any assignment at this time.

The above description applies only in a noncoordinating solvent and many of the solvents examined are not inert with respect to these complexes. Mixed hexanes and methylcyclohexane are inert. Halogenated solvents, acetonitrile, tetrahydrofuran, and even toluene are not. When compared to [Zn(mesdpm)₂], the new gallium(III) and indium(III)

(51) Strickler, S. J.; Berg, R. A. *J. Chem. Phys.* **1962**, *37*, 814.

(52) Turro, N. J. *Modern Molecular Photochemistry*; Benjamin/Cummings, Inc.: Menlo Park, CA, 1978.

Group 13 Dipyrrinato Complexes

complexes were slightly more stable. [Zn(mesdpm)₂] was found to be unstable over weeks even in noncoordinating solvents. The combination of the well-behaved optical properties reported here along with the stability of the complexes suggest that further “tuning” of the structure might well afford some improvement in the fluorescent quantum yield, but even at the present level, one can visualize applications for this new class of dipyrrin-based fluorophores.

Acknowledgment. We thank Prof. Arnold L. Rheingold (U.C.S.D.) and Dr. Yongxuan Su (U.C.S.D.) for assistance with the X-ray and mass spectrometry data collection, respectively. We thank Dr. Drew L. Murphy for synthetic assistance with [Ga(4-cydpn)₃]. This work was supported by the University of California, San Diego, the donors of

the American Chemical Society Petroleum Research Fund, and the National Science Foundation (CHE-0546531). This research was supported in part by W. M. Keck Foundation through computing resources at the W. M. Keck Laboratory for Integrated Biology II. J.R.S was supported by an NIH training grant (T32 HL007444-25) and V.S.T. was supported, in part, by a U.C.S.D. Summer Research Fellowship. S.M.C. is a Cottrell Scholar of the Research Corporation. D.M. thanks the late Prof. K. Wilson and the late Prof. B. Zimm.

Supporting Information Available: Figures S1–S6; Complete ref 28; X-ray crystallographic data in CIF format. This material is available free of charge via the Internet at <http://pubs.acs.org>.

IC061581H